Rate Dependent Rupture of Solid-Supported Phospholipid Bilayers

by

Sarah S Ng

Submitted to the Department of Materials Science and Engineering in Partial Fulfillment of the Requirements for the Degree of

Bachelor of Science

at the

Massachusetts Institute of Technology

May 2006
[June 2006]

Signature of Author.....
Department of Materials Science and Engineering
May 22, 2006

Certified by.....
Christine Ortiz
Associate Professor of Materials Science and Engineering
Thesis Supervisor

Accepted by.....
Caroline A. Ross
Professor of Materials Science and Engineering
Chair, Department Undergraduate Committee

Rate Dependent Rupture of Solid-Supported Phospholipid Bilayers

by

Sarah S. Ng

Submitted to the Department of Materials Science and Engineering on May 22, 2006
in Partial Fulfillment of the Requirements for the Degree of Bachelor of Science in
Materials Science and Engineering

ABSTRACT

An experimental study on solid-supported phospholipid bilayers was performed in order to investigate rate-dependent behavior of force and probability of bilayer rupture. 1-palmitoyl-2-oleoyl-*sn*-glycero-3-phosphocholine (POPC) solid-supported lipid bilayers were created on mica using vesicle fusion technique and then ruptured normal to the surface using a silicon nitride cantilever tip (radius≈80nm). High resolution force spectroscopy was performed using the Molecular Force Probe (1D) to obtain force versus distance curves between the tip and substrate, varying the rate of penetration between a range of 250 nm/sec to 8.0 μm/sec. Statistical analysis was used to find distributions for average yield distance and yield force at different rates to find correlations in our data. Lastly, experimental data was compared to proposed theoretical models that describe rupture probability as a function of activation energy.

A two yield force profile on approach was achieved with consistency at all rates. The yield forces occurred at statistical significant distances of around 4 nm and 9 nm, which are consistent with bond calculations of the phospholipid. However, no relationship was found between force and tip velocity within the range of experimentation. Because rupture occurred even at the lowest penetration rates, activation energy for bilayer rupture appears to be quite low. Moreover, this also suggests that standard atomic force microscopy imaging stimulates perturbation of the surface, leading to imprecise characterization. Further investigation into a larger range of tip velocities, as well as the role of tip radius on rupture probability are recommended for a greater quantitative understanding of solid-supported bilayers.

Thesis Supervisor: Christine Ortiz
Title: Associate Professor of Materials Science and Engineering

LIST OF EQUATIONS, FIGURES, AND TABLES

ACKNOWLEDGEMENTS

I would like to thank Professor Christine Ortiz and Jae Hyeok Choi for their guidance on this project. I would also like to thank Sheree Michelle Beane, Cathal Kearney, and Haile Negussie for their additional assistance, and as well as the MIT Institute of Soldier Nanotechnologies and Irvine laboratory for the use of their facilities. This research project is funded in part by the National Science Foundation and the MIT Undergraduate Research Opportunities Program.

TABLE OF CONTENTS

1. INTRODUCTION

1.1 Solid-Supported Lipid Bilayers: Classification and Significance

Biological cell membranes have prominent roles in cell life. They act as the gateways for ions and molecules between the interior of cells and their surroundings, and control the transfer of information in and out. Via integrated proteins, membranes participate in both intra- and extra-cellular processes, playing important roles in the regulation of cell behavior and the organization of tissues in cells. Biological membranes are highly complex and dynamic assemblies, but are based in a two-dimensional space made of lipid molecules, which are held together by hydrophobic interactions, and self-assembled as a continuous bilayer[21].

More recently, the deposition of model membranes on solid supports has become a very popular means for studying cell membrane characteristics[22]. The growing interest in introducing lipid membranes on surfaces has been cultivated by the development of greater surface-sensitive characterization techniques, advanced surface patterning methods, and liquid handling systems[21]. Solid-supported lipid bilayers (SLBs), which come in many variations[5,11,16], are a self-assembly of amphiphilic phospholipids onto a hydrophilic surface such as mica or silica. These systems are highly fluidic yet stable and are achieved due to hydrophilic interactions that exist between the head groups of the phospholipids and the surface, as well as hydrophobic interactions between hydrocarbon tails of the lipid molecules. Additionally, a thin water layer of approximately 10-20 Å often exists between the solid support and the bilayer. Consequently the lipids have the freedom to diffuse laterally, which preserves an important dynamic property of biological membrane[21].

Because solid-supported lipid bilayers behave as such useful models of biological cell membranes, they can be utilized to study membrane characteristics and processes. Considering them as a monolayer surface, lipid bilayers are

intriguing to study because they have coherence as elastic thin films, yet their high molecular nature makes the surface easily susceptible to both rupture and quick restoration to their natural state. They have been proven valuable in a broad collection of both physical investigations and biological research. These applications range from the study of membrane structure thermodynamics, the determination of immune cell response mechanisms, to the development of biosensors using membrane-based integrin receptors[9,14]. Additionally, because these supported bilayers allow free lateral diffusion of lipid molecules and associated membrane proteins, these bilayer systems are also well-suited to analyze lipid domain function[21].

1.2 Lipid Bilayer Characterization Techniques

Because lipid bilayers exist as water-based films, characterization techniques are limited to those that can operate in aqueous environments. Thus far, researchers have used ellipsometry and surface plasmon resonance (SPR) to study membrane properties[17,19,31]. However, atomic force microscopy (AFM) is by far the most frequently used tool for characterizing membrane properties due to its ability to create high resolution images in aqueous environments. Using these imaging capabilities, AFM has been used for a number of applications investigating bilayers, including structure and stability[10], rupture[15], height[7], phase transitions[4,28], consequences of membrane protein incorporation[6,30], interaction on polymer beds[32]

However there may be drawbacks in using atomic force microscopy imaging to characterize lipid bilayers. Due to the nature of the functionality of the AFM, localized instabilities over the lipid surface make the possibility of surface disruption from the cantilever probe tip likely, even when using tapping mode. For example, the majority of references show bilayer height (with varying phospholipid monomers) to be less than 5 nm, though, as show in the experimental section, bond calculations indicate that these values may be less than reality. Additionally, the sensitivity of

bilayers due to its molecular nature poses more questions about how much disturbance occurs used during AFM imaging, what minimum forces cause this disturbance, (is this force less than the setpoint for needed to obtain good imaging), and what induces full rupture through the surface of the bilayer. Therefore we would like to utilize another method of characterizing these bilayers, in order to investigate these questions, especially concerning the force thresholds that bring about surface rupture in bilayers, and what variables dictate this force.

1.3 High Resolution Force Spectroscopy

Force measurements can be obtained in order to better interpret AFM images of solid-supported bilayers. These force measurements are obtained with high resolution force spectroscopy (HRFS), using either the atomic force microscope (AFM) or an instrument of a similar quality, the Molecular Force Probe™ (MFP) (Asylum Research, Inc). The MFP's 1-Dimensional functionality does not allow for imaging, but rather solely focuses on measuring surface forces as a function of distance away from the surface. A cantilever tip is brought toward the surface until it comes into contact. Repulsive forces are measured by the deflection of the cantilever upward as it approaches the surface. When the cantilever and surface reach a contact regime, the force between the two goes toward infinity.

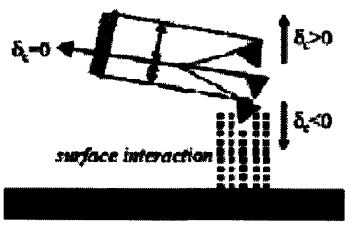

Figure 1.1 Deflection of cantilever in response to intermolecular interactions with the surface. Adhesion is observed when $\delta_c < 0$, repulsion when $\delta_c > 0$.

Upon this, the cantilever and surface are retracted from each other and a corresponding retraction curve is evaluated. If adhesion is present between the tip and surface at a given distance, the region will appear to have negative force.

On typical force curves for lipid bilayers, no interaction is observed at distances much larger than the film thickness. As the tip moves towards closer distances, it experiences short-range repulsive force and the film is elastically compressed. In this context, "elastic" refers to the region before the tip ruptures the film, where the retract curve is identical to the approach curve[2]. Once a threshold force is attained, the tip makes a jump to contact down to the solid support, with little or no additional force for penetration.

1.3 Force-dependent bilayer rupture: Theory

Due to the discrete nature of phospholipid thin films, its observed rupture must be taken as a statistical process. The tip has a certain probability P(F) to break through the layer at a given applied force, which increases with increasing force and applied pressure. Thus, a distribution of forces at which a bilayer yields exist. Earlier work by Butt et al.[2,15] attempts to quantitatively describe this probability. The aim of this theory is to calculate this distribution of yield forces and relate microscopic parameters to measurable quantities.

To begin with, an energy barrier must be overcome for the formation of a hole in the layer, which is large enough to initiate tip penetration. This activation energy decreases with increasing applied force:

$$\Delta U = U(r_C) = \frac{2\pi^2\Gamma^2 R}{F - 2\pi RS}. \qquad \textbf{Equation 1.1}$$

where R is the tip radius, Γ is the line tension of the film associated with the unsaturated bonds of the molecules at the periphery of the hole where penetration

occurs, S is the spreading pressure or the energy per unit area gained by the layer when spreading into the gap between the tip and substrate, and F is the applied force, that changes with time as the tip penetrates the bilayer surface. A derivation of this relationship and the following are found in the referenced publications. Generally, the profile, as schematically represented in Figure 1.2, changes with the force applied. As pressure increases, the activation energy is reduced even though the tip is still positioned on top of the film.

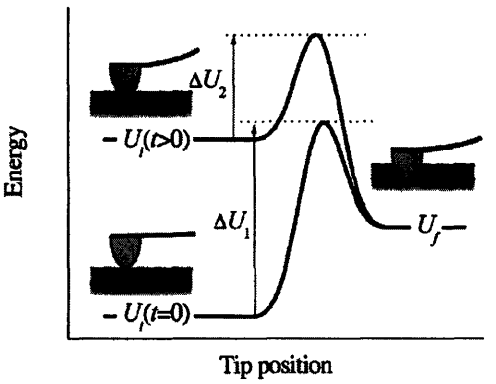

Figure 1.2 Schematic representation of the activation required for bilayer penetration. *Butt et al. Physical Review 2002 66 031601-2*

Two separate models of the rupture process exist. The first, named the continuum nucleation model, treats the bilayer as a continuous elastic layer which yields at a certain stress. The representation does not take into account the molecular nature of the layer. In particular, it ignores the fact that the interaction of the phospholipids in the lateral direction is generally different from their interaction in the normal direction. The probability distribution could be expressed by the force-dependent activation energy and approaching velocity *v*.

$$\ln P(F) = -\frac{A}{Kv}\int_{F_S}^{F} \exp\left(-\frac{2\pi^2\Gamma^2 R}{F'-F_S}\right)dF' \qquad \textbf{Equation 1.2}$$

for $F > F_s$, $P=1$ for $F \leq F_s$, and where A represents the tip frequency, v, the initial loading rate, K, the spring constant of the cantilever, and where $F_s = Kvt = 2\pi RS$, or

the initial force at penetration. Here, P is the probability to find the tip still on top of the layer (penetration failure)

The alternative is the discrete molecular model. In the molecular model, each molecule in the film has certain binding sites which are energetically favorable. These binding sites might be formed by the substrate or by the surrounding molecules. To jump from the initial position into an adjacent free position a potential energy barrier has to be overcome. In the absence of the tip adjacent binding sites are energetically equivalent. When the tip is pressed onto the film a pressure gradient is applied which increases the energy of the molecules. The pressure is maximal in the center of the tip and it decreases with increasing radial distance until it becomes zero at the contact periphery. The probability of rupture failure following the molecular model can be described as follows:

$$\ln P = -\frac{k_0 F_T}{K\nu}\left(e^{F/F_T} - 1\right)$$

Equation 1.3

where

$$F_T \equiv \frac{4\pi h R k_B T}{V}$$

Equation 1.4

and k_0 is the rate of spontaneous hole formation, and V is the activation volume.

2. MATERIALS AND METHODS

2.1 Formation of solid-supported lipid bilayer

Solid-supported lipid bilayers were created using vesicle fusion technique. This technique involves the formation of lipid vesicles in solution, introducing them to a hydrophilic surface, and allowing the vesicles to spontaneously adsorb onto the surface, where the phospholipids rupture and spread into a homogenous bilayer.

Lipid Vesicle Preparation:

Phospholipid 1-palmitoyl-2-oleoyl-*sn*-glycero-3-phosphocholine (POPC) was purchased from Avanti Polar Lipids (Alabaster, AL). A 10 mM solution of POPC was prepared in organic solvent, chloroform. The POPC/chloroform solution was then mixed with a 9:1 chloroform:methanol solution to produce a 3mg/mL lipid solution. 2 mL of the lipid mixture was place under a flow of argon to allow the chloroform to evaporate, leaving a lipid film on the walls of a round beaker. The sample was then lyophilized under for at least 8 hours. The lyophilization process freeze dried and dehydrated the sample under high vacuum, serving to extract small contaminants from the sample. After lyophilization, 2 mL of degassed 0.1 M Tris buffer was added. The lipids in solution were sonicated for approximately 30 minutes to facilitate the formation of small unilamellar vesicles (SUVs). Lastly, the mixture was centrifuged at 9000 rpm, in 5 mL tubes on a 50.1 Ti swinging rotor, so that large vesicles were separated out. The suspended vesicles in solution were extracted.

Vesicle Characterization and Formation of Bilayer:

Previous measurements using quartz crystal microbalance with dissipation monitoring (QCM-D) and surface plasmon resonance (SPR)[20] have shown that isolated vesicles need to remain intact when absorbed onto the surface, and that a certain surface density of vesicles (critical vesicular coverage) is required to initiate the decomposition of surface-bound vesicles into bilayer patches. These two

conditions are in large part fulfilled by controlling the density of the lipid solution applied to the surface, and the size of the vesicles. A spectrophotometric reading was performed using a 1:9 ratio of POPC vesicle solution to 0.1 M Tris buffer to determine the density of particles in solution. To determine the distribution of vesicle diameter, dynamic light scattering (Brookhaven Instruments Limited™) was also performed with an approximately 3:1 mixture of de-ionized water and vesicle solution. A distribution of vesicle diameters ranging from 60 to 100nm was taken as optimal for vesicle spreading over the surface.

After vesicle characterization, the solution was diluted to 0.1mg/mL. 100 µL of vesicle solution was then introduced over a ~1 cm^2 sample of mica, and placed in a 40°C environment for thirty minutes to facilitate the spreading of vesicles over the surface, as Figure 2.1 depicts.

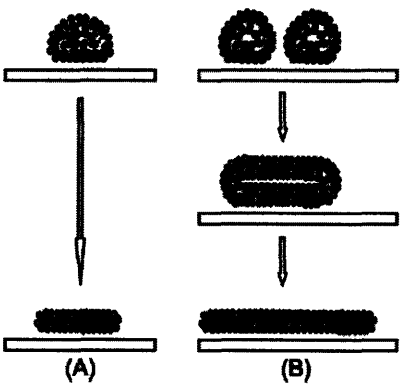

Figure 2.1 Vesicle fusion technique. *Richter et al. Langmuir 2006 (22) p.3499*

2.2 Atomic Force Microscopy Imaging

Bilayers were imaged using the Atomic Force Microscope in fluid. Imaging was performed on the bilayer in 0.1 M Tris buffer in contact mode with a silicon nitride cantilever tip. The first imaging is taken at a 5 µm x 5 µm scan size. The scan size is then changed to 1 µm x 1 µm and the setpoint force is increased well beyond what is needed to get an image. This high-setpoint scan creates strong

abrasion against the surface with enough force to scratch off the lipid layer in the area. Lastly, the surface is re-imaged at the original 5 μm x 5 μm area, and section analysis is done. The height difference between the undisturbed area and scratched section would be an approximate height estimation of the bilayer using this imaging technique.

2.3 Height Analysis by Bond Calculation

Additional height information was obtained by acquiring a rough calculation of POPC's height using the bond lengths in Table 2.1. Geometric bond angles were taken into account.

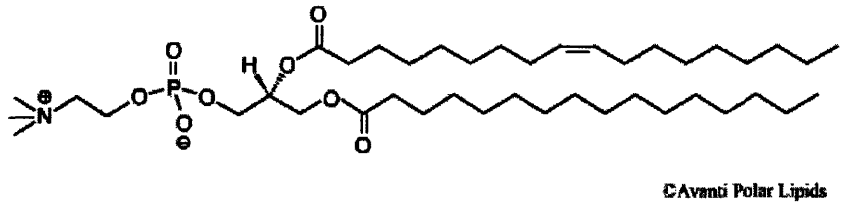

Figure 2.2 Structure of 1-Palmitoyl-2-Oleoyl-*sn*-Glycero-3-Phosphocholine (POPC)

Bond	Bond Length (pm)
C-C	154
C-O	143
C-N	143
C=C	133
O-P	163
C-H	107

Table 2.1 Bond lengths used to estimate height of phospholipid POPC

High Resolution Force Spectroscopy:

Force characterization was done using the Molecular Force Probe 1D™ (MFP 1D). The reason MFP was chosen was because it is more adapted than the AFM to experiments done in open fluidic environments (piezo and electric components lie above rather than below sample) and to larger sample sizes.

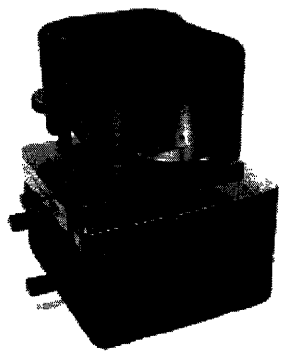

Figure 2.3 Molecular Force Probe™

Experiments were performed in 0.1M Tris buffer, using a Veeco 0.06 N/m silicon nitride probe tip. Before each experiment, the inverse optical lever sensitivity (IOLS), thermal spectrum, and spring constant of the cantilever tip were determined and recorded. Force versus distance curves were taken at a variety of locations on each sample at a tip rate of 1.0 μm/s. Whenever a stable bilayer was located by a consistent yield force or yield forces on the approach curve, the tip rate was modified. Data was taken within rate ranges of 250 nm/s to 8.0 μm/s.

Comparison to Theoretical Models

Equations for probability of rupture cannot be evaluated analytically, and were therefore evaluated numerically and plotted, plugging in values based on our experimentation as well as from references.

A = 5kHz; S = 9.5 mN/m; $\Gamma = 3.5 \times 10^{-12}$ N/m; R = 50 nm; $F_s = 2\pi RS$; K = 0.07 N/m; v = 2 μm/s.

3. RESULTS AND DISCUSSION

3.1 Lipid Bilayer Characterization

The initial goal of this research was to characterize the POPC lipid bilayer on mica surface. This was to show that a bilayer did indeed exist on the surface, and to demonstrate one technique of measuring bilayer height using the Atomic Force Microscope. AFM images demonstrated that a phospholipid bilayer did successfully spread over the surface, though perhaps not as homogenously as desired. (Figure 3.1a)

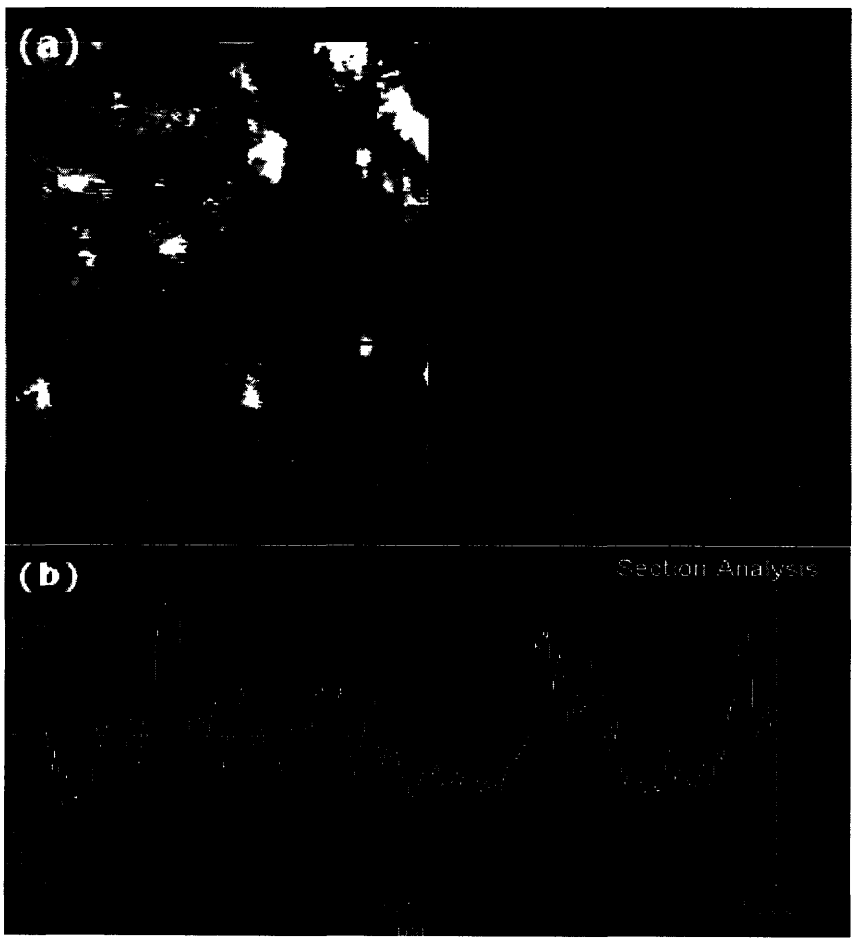

Figure 3.1 a) Atomic Force Microscopy image of POPC phospholipid bilayer. Center, 1 μm^2 region was "scratched out" using a high setpoint raster. Height image is on the left, deflection image is on the right b) Section Analysis. Height is within 2-3 nm.

Using a high setpoint in contact mode, we were able to "scratch out" the center section of the bilayer. Section analysis across this region showed that the relative height difference was less than 3 nm. (Figure 3.1b) This estimation is on the shorter end; however it is in agreement with references showing that the bilayer is less than 5 nm.

Bond calculation of 1-Palmitoyl-2-Oleoyl-*sn*-Glycero-3-Phosphocholine (POPC) resulted in a quite dissimilar value than height taken from AFM imaging. One POPC lipid was calculated to be approximately 4 nm in length, making a bilayer up 8 nm. This does not take into account the flaccidity of the lipids in its natural state. However, the discrepancy is drastic enough that addition investigation is necessary.

3.2 Rate-Dependent Force Spectroscopy

Force curves obtained by High Resolution Force Spectroscopy resulted in quite a range of data. Figure 3.2 depicts two typical force profiles. On approach, we were able to extract both the distance from the surface at which the bilayer yields, as well as the force required for the bilayer to yield. It is hypothesized that when two yield forces and distances are evident (3.2a), it is an indication that a higher force is required to break through the bottom phospholipid layer onto the solid support after the tip penetrates through the first phospholipid layer in the film. However when only one yield force (3.2b), this suggests that the initial force required to break through the film is adequate to rupture all the way down to the solid support. This theory is supported by the fact that the average yield distance of rupture is comparable to the yield distance of the first breakthrough in the two-force profile.

For simplicity sake, the lower yield force from longer distance will be referred to as the first breakthrough force. The higher yield force at shorter range will be referred to as the second breakthrough force.

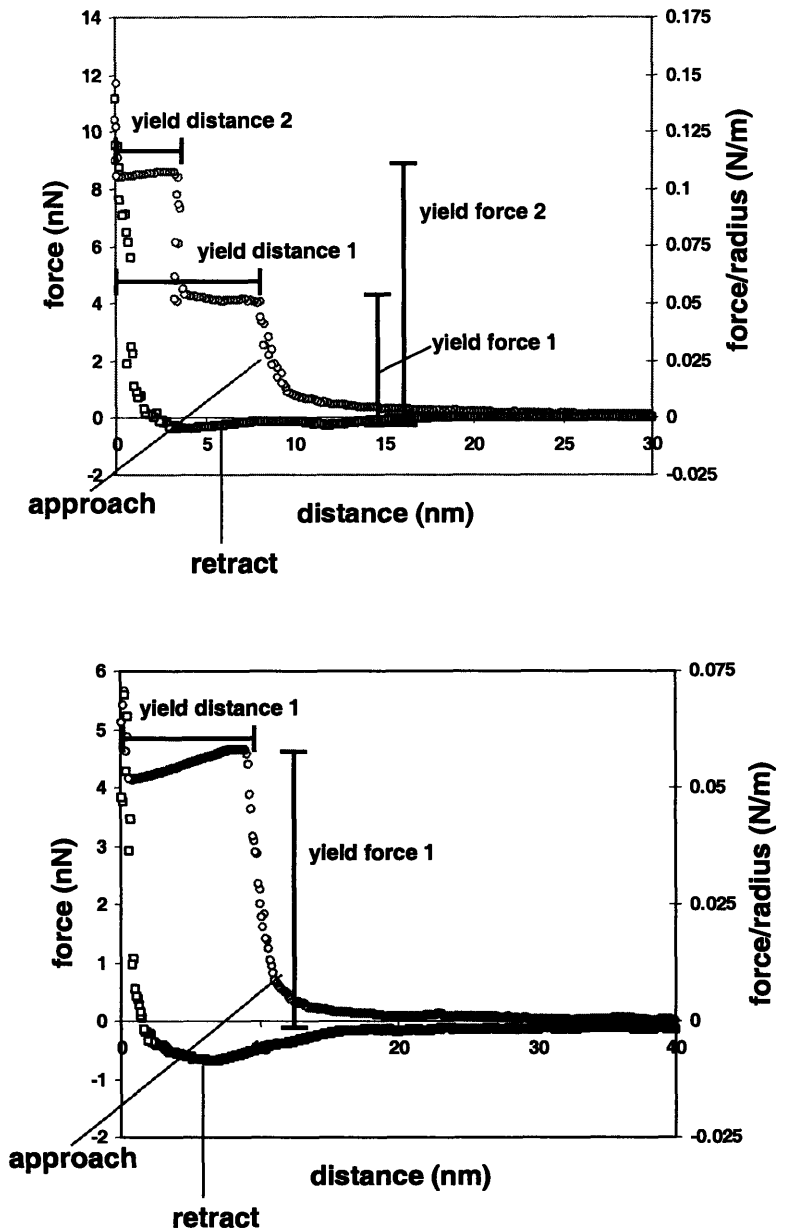

Figure 3.2 Typical force profiles obtained by High Resolution Force Spectroscopy experiments on solid-supported phospholipid bilayer. (a) approach curve with two yield forces (b) approach curve with one yield force

Lastly, there are also instances in which no step force is observed (not shown). This occurrence signifies one of two scenarios. The first possibility is that there is no bilayer at that location and the tip merely approaches and retracts off of the solid support. The mica used is both atomically flat and inert. The second possibility is

that the tip failed to penetrate through the bilayer before it retracted. In other words, there was not enough activation energy in that force to induce rupture on the thin film, and is denoted as a rupture failure. Rupture failure was distinguished between bilayer absence when a bilayer was already established at a given location by preceding runs. Ultimately, at any given experimental state, a distribution of varying force profiles is observed. Therefore, statistical analysis was used in order to draw more conclusive correlations between variables.

A very strong correlation between yield force and yield distance was obtained over the range of all tip velocities from 250 nm/s – 8.0 μm/s.

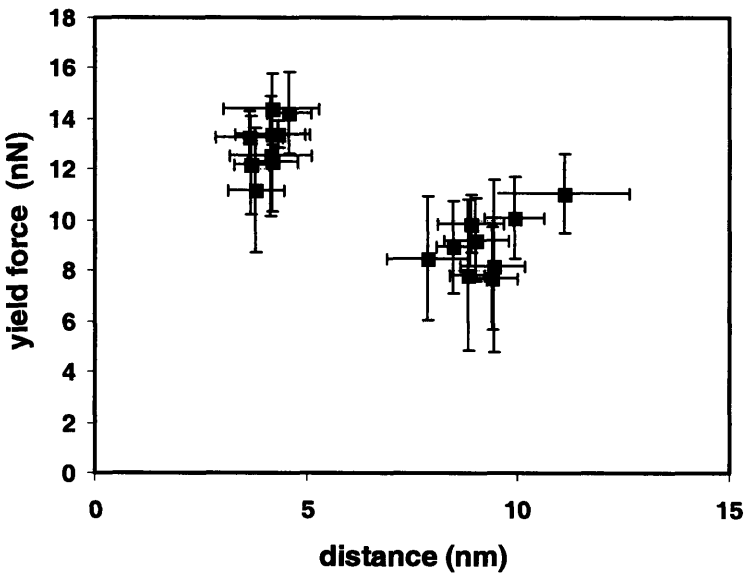

Figure 3.3 High resolution force spectroscopy: average yield force versus yield distance for n=209, POPC lipid bilayer on mica.

In Figure 3.3 we see that at higher yield forces, forces over 10 nN correlated with the second step force (shorter distance, larger yield force) at a yield distance averaging around 4nm. Lower yield forces, primarily below 10 nN, showed a much greater yield distance of around 9nm, which corresponds with the first step force

(longer distance, smaller yield force). Figure 3.4 lays out a histogram of the yield distance alone. Two distinct distributions approaching Gaussian form emerge are evident from this data. Furthermore, we see that the distribution of yield distances of the second breakthrough has a more even spread than that of the first breakthrough. This makes sense when considering the more restricted mobility of the bottom lipid layer as compared to the top lipid layer. These correlation between yield force and yield distance seems to support the bond calculations for POPC bilayer height.

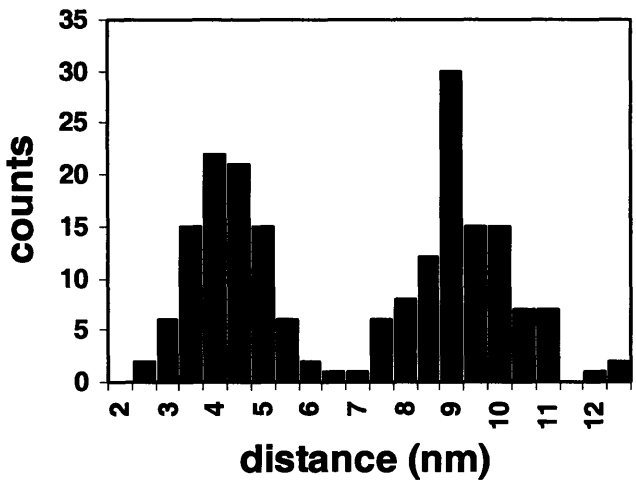

Figure 3.4 Distribution of yield distances over a tip velocity range of 250 nm/s – 8.0 μm/s; n=209

The distribution of yield forces (Figure 3.5) does not show the same bimodal distribution that the distribution of yield distances showed. Rather, the distribution is wider, and inconclusively distributes around 12 or 13 nN.

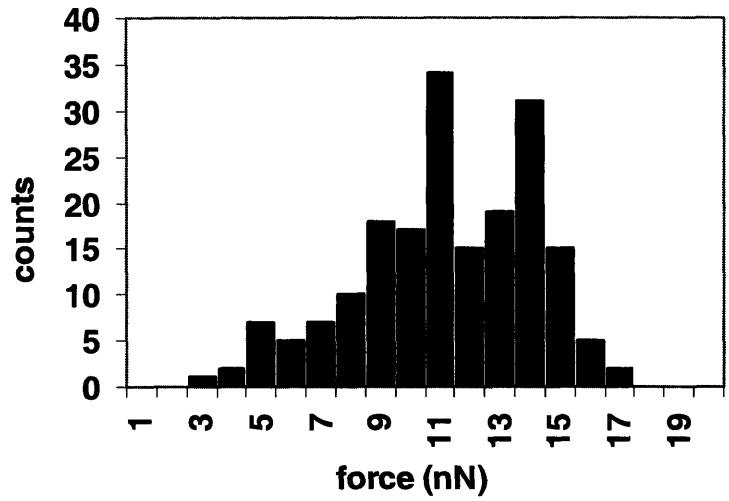

Figure 3.5 Distribution of yield forces over a tip velocity range of 250 nm/s – 8.0 μm/s; n=209

However, because there is such a strong discrepancy between the average yield distance at yield forces less than 10 nN and those at yield forces greater than 10 nN, it cannot be assumed that this distribution will narrow toward a point where one of the breakthrough forces would be eliminated.

When only one breakthrough force was observed, breakthrough almost always occurred at the greater distance (8-9 nm) from the surface (Figure 3.2b). Thus the breakthrough is labeled as a first yield force rather than a second. This supports the idea that the tip is indeed rupturing through one bilayer, approximately 9 nm in height. We investigated whether there was a correlation between the first yield force on a single breakthrough, and the first yield force when two breakthroughs were observed. It was expected that the first yield force on a single breakthrough would perhaps be higher, hence the increased probability of the tip to possess enough activation energy to rupture through the entire bilayer in one fluid penetration. However, single rupture force was found to be 7.0 +/- 2.5 nN, whereas the first yield force on duel breakthrough was found to be 9.4 +/- 2.1 nN. One possible explanation is simply that there were relatively few instances of single

rupture force profiles observed compared to the two breakthrough force profiles. Therefore more data is required to draw a conclusion about the relationship between the first breakthrough yield force in one-breakthrough profiles versus that of double-breakthrough profiles.

In this research, one of our main goals was to see if there was a correlation between tip velocity and breakthrough force. This was so a relationship could be made between rate and the activation energy required to breakthrough a phospholipid bilayer using the aforementioned theory between force and activation energy. Within the velocity ranges used, however, no relationship between force and rate was achieved. This can be seen in Figure 3.6.

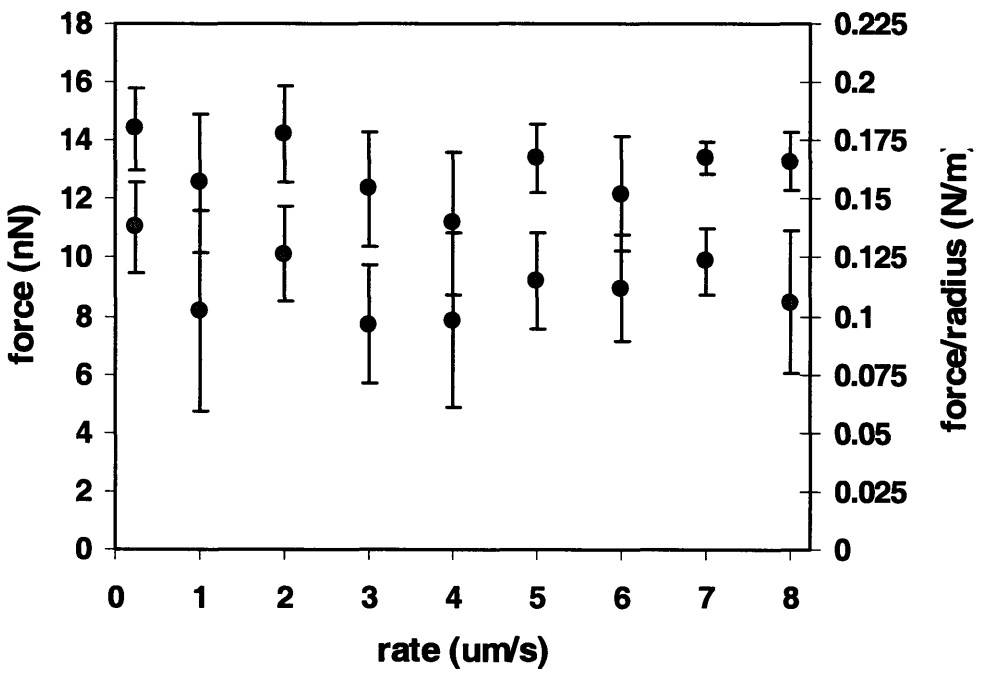

Figure 3.6 Yield force as a function of tip velocity. Black circles represent second breakthrough force. Grey circles represent first breakthrough force.

While there does seem to be distinction between the first and second yield force for each rate, as discussed earlier, no correlation was observed in terms of

increasing force as the tip velocity was increased. It should be considered, however, that more experimentation should be done for further clarification. Additionally, it is possible that a relationship may be observed if measurements were taken at a greater range of rates, for example up to a magnitude higher tip velocity. The experiments performed in this research were somewhat limited to the resolution, in terms of being able to see a yield force at the greatest number of points per second available with the software used (Igor Pro v.5). Even at 20,000 points/sec (limit), details on the approach curve were more difficult to observe. However obtaining a force dependence profile on tip velocities up to 100 μm/s would be greatly beneficial.

3.3 Comparing Experimental Data to Theoretical Models

In evaluating our models from reference, both the continuum nucleation model and molecular model are observed and analyzed best as log plots because the constants inflated the magnitude of the exponential drop considerably.

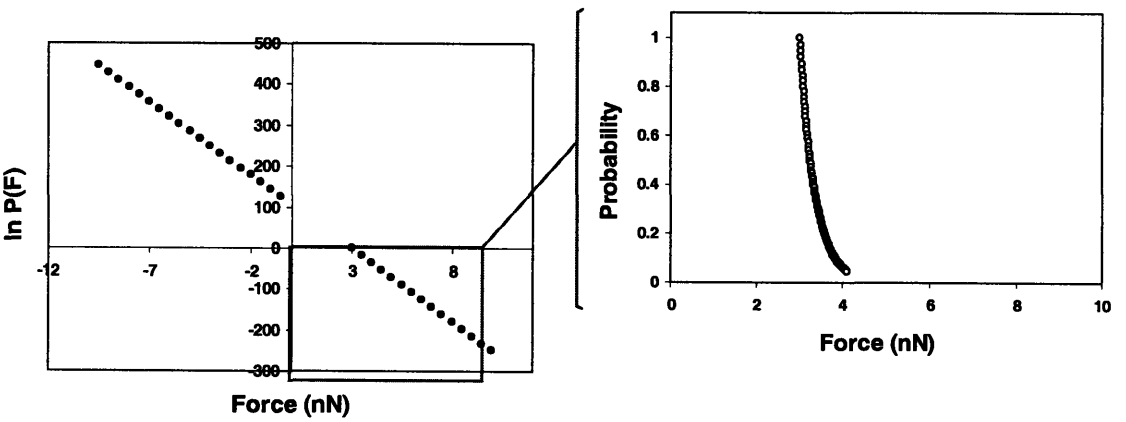

Figure 3.7 Plot of continuum nucleation model: $\ln P(F) = -\frac{A}{K\nu}\int_{F_S}^{F} \exp\left(-\frac{2\pi^2\Gamma^2 R}{F'-F_S}\right)dF'$: probability of rupture failure as a function of applied force A/Kν constant out front makes the rapid exponential drop over span of 1 nm.

Furthermore, because the integrals involved did not lead to simple analytical solutions, they had to be solved numerically. The continuum nucleation model is plotted in Figure 3.7, where P is the probability of rupture failure. The probability of rupture at $F < F_S$, which signifies the initial required force (Kvt), is defined to be 1. For $F > F_S$, there is a rapid exponential drop. Therefore the probability that rupture will occur grows to 1, over a span of only 1 nN approximately. F_S, where $F_S = 2\pi RS$, thus acts as more of a threshold of rupture occurrence, rather than the initiation of an integrative profile. Based on the parameters we used, F_S is quite small. Therefore the activation energy required for rupture is not great. This makes sense if we re-examine Equation 1.1 for activation energy. Since F_S turns out to be so small, the differential in force will tend to be large, decreasing the overall activation energy required. Due to uncertainty about the real values of line tension Γ and spreading pressure S, the actual ΔU values were not calculated. Currently these values are not measured, only fitted to experimental data. Thus a more effective way to determine these parameters is still required to evaluate the relevance of the model.

The discrete molecular model was not evaluated because the F_T parameter needed in the equation is determined by obtaining constants from the log relationship between percent penetration failure and tip rate. In plotting this data, we were able to attain a best-fit log regression. However the least square values, R, were too large to draw significant data from these graphs. An example of one of these plots is shown in Figure 3.8.

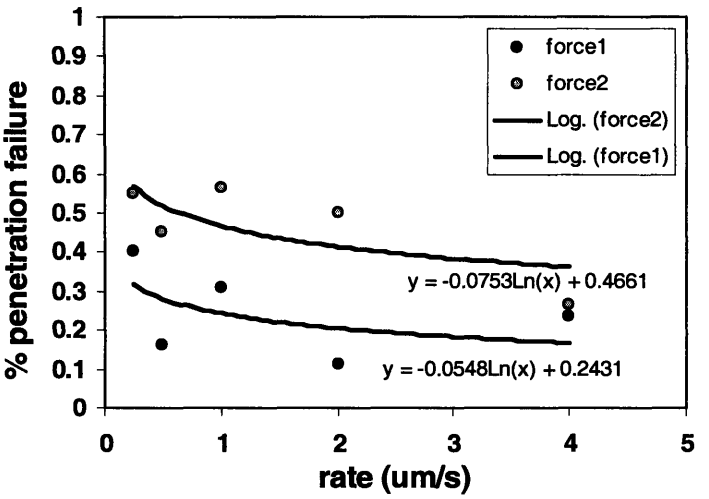

Figure 3.8 Percent penetration failure as a function of tip velocity

3.4 Further Investigations

One variable that was not and has not been investigated is the role that tip radius plays in force characterization of lipid bilayers. In this research, the two-step force profile seemed to be obtained more consistently than in other works. It is possible that a larger tip radius is the cause. Scanning electron microscopy (SEM) imaging was performed on the silicon-nitride cantilever tips used during experimentation. These images revealed that the probe tip radiuses were a bit larger than expected—around 80 nm instead of 50 nm. The theory that a larger tip radius would increase the probability of a two step profile makes sense. If we think about the need for an opening in the bilayer to spontaneously form for a tip to penetrate through the surface, a larger opening would be required for a rounder tip to rupture through the entire surface than a sharper tip would. Furthermore, the equations describing the probability of rupture failure also indicate a larger radius will result in a higher probability of failure occurrence.

Using parameters obtained experimentally and from reference, we saw that the distribution for the exponential drop in probability of rupture failure was barely more than 1 nN. Assuming these parameters, especially for spreading pressure and line tension are on the right order of magnitude, the "elastic" region of the bilayer force profile should be further investigated. Specifically, this could entail finding which external variables dictate bilayer elasticity, and how this elastic range can be extended to create a bilayer of greater stability.

CONCLUSION

In this research, we were able to consistently obtain a two-yield force profile with a strong correlation between the yield distances and breakthrough force. The implications of are intriguing. We see what seems to be a discrepancy in lipid bilayer height characterization under normal atomic force microscopy imaging methods. While all references found show height of bilayer as under 5 nm, high resolution force spectroscopy experimental data from this research indicate that the bilayer may be closer to a height of 8 nm. Additionally, this is consistent with height analysis from bond calculation estimates. Increased evidence of this occurrence as compared to previous work may be related to tip radius, and it is recommended that this should also be investigated. Though it was not explored in this work, double yield forces would accommodate separate activation energies ΔU_1, ΔU_2 and rupture probability $P_1(F)$, $P_2(F)$ in the same system and could be solved as such.

No positive relationship between rate and yield force was observed on either breakthrough forces in either one or two yield force profiles. Our force and rate dependent experiments further support the theory that the bilayer is greater than indicated by atomic force microscopy imaging. Rupture was observed consistently even at low tip velocities down to 250 nm/s. Therefore even at low penetration rates, there is enough force to break through the bilayer. However, these results seem consistent with our plot of the continuum nucleation equation, which illustrates a sharp increase in rupture probability over a range of about 1 nN, after the initial required force F_S. With $F_S = 2\pi RS$, where spreading pressure S = 9.5 mN/m, and R = 50 nm, F_S is only 3 nN of force. Larger radii tips should be examined to see if there is a correlation between rupture probability and tip radius. In theory, increasing the size of the tip radius will increase F_S and therefore raise the threshold force needed for rupture.

Additional suggestions for further work include doing a more thorough analysis of rate dependence over several locations in the bilayer, as well as an investigation of whether rate dependence becomes more evident as rate is increased more dramatically than done in this work. Lastly, a molecular dynamics simulation of a solid-supported lipid bilayer system could be extremely beneficial in determining which forces govern phospholipid bilayer rupture and how they govern. This would also provide a never-before obtained visual of the bilayer system, and rupture outcomes could be generated by adjusting the parameters.

With further investigation and analysis, lipid bilayer rupture can be quantitatively modeled, thereby offering us a better understanding of these unique thin films.

REFERENCES

1. Benz M, G. T., Chen N, Tadmor R, Israelachvili J (2004). "Correlation of AFM and SFA Measurements Concerning the Stability of Supported Lipid Bilayers." Biophysical Journal 86: 870-879.

2. Butt H-J., F. V. (2002). "Rupture of molecular thin films observed in atomic force microscopy. I. Theory." Phys. Rev E 66: 031601.

3. Butt H-J., C. B., K. M. (2005). "Force measurements with the atomic force microscope: Technique, interpretation and applications." Surface Science Reports 59: 1-152.

4. Charrier A, T. F. (2005). "Main Phase Transitions in Supported Lipid Single-Bilayer." Biophysical Journal 89: 1094-1101.

5. Chiu SW, J. E., Subramaniam S, Scott HL (1999). "Combined Monte Carlo and Molecular Dynamics Simulation of Fully Hydrated Dioleyl and Palmitoyl-oleyl Phosphatidylcholine Lipid Bilayers." Biophysical Journal 77: 2462-2469.

6. Domenech O, M.-M. S., Montero M, Hernandez-Borrell J (2006). "Surface planar bilayers of phospholipids used in protein membrane reconstitution: An atomic force microscopy study." Colloids and Surfaces B: Biointerfaces 47: 102-106.

7. Dufrene YF, B. T., Schneider J, Barger W, Lee GU (1998). "Characterization of the physical properties of model biomembranes at the nanometer scale with the atomic force microscope." Faraday Discuss 111: 79-94.

8. Grandbois M, C.-S. H., Gaub H (1998). "Atomic Force Microscope Imaging of Phospholipid Bilayer Degradation by Phopholipas A2." Biophysical Journal 74: 2398-2404.

9. Groves JT, U. N., Boxer S (1997). "Micropatterning Fluid Lipid Bilayers on Solid Supports." Science 275: 651-653.

10. Hui SW, V. R., Zasadzinski JA, Israelachvili JN (1995). "The Structure and Stability of Phospholipid Bilayers by Atomic Force Microscopy." Biophysical Journal 68: 171-178.

11. Janshoff A, R. M., Gerke V, Steinem C (2001). "Visualization of Annexin I Binding to Calcium-Induced Phophatidylserine Domains." ChemBiochem 7/8: 587-590.

12. Janshoff A, S. C. (2001). "Scanning Force Microscopy of Artificial Membranes." ChemBiochem 2: 798-808.

13. Jass J, T. T., Puu G (2000). "From Liposomes to Supported, Planar Bilayer Structures on Hydrophilic and Hydrophobic Surfaces: An Atomic Force Microscopy Study." Biophysical Journal 79: 3153-3163.

14. Kung L. A., L. K., H. J., B. S. (2002). "Patterning Hybrid Surfaces of Proteins and Supported Lipid Bilayers." Langmuir 16: 6773-6776.

15. Loi S., G. S., V. F., Butt H-J. (2002). "Rupture of molecular thin films observed in atomic force microscopy. II. Experiment." Phys. Rev. E 66: 031602.

16. Merino S, D. O., Diez-Perez I, Sanz F, Montero M, Hernandez-Borrell J (2005). "Surface thermodynamic properties of monolayers versus reconstitution of a membrane protein in solid-supported bilayers." Colloids and Surfaces BL Biointerfaces 44: 93-98.

17. Meuse CW, K. S., Majkrzak CF, Dura JA, Fu J, Connor JT, Plant AL (1998). "Hybrid Bilayer Membranes in Air and Water: Infrared Spectroscopy and Neutron Reflectivity Studies." Biophysical Journal 74: 1388-1398.

18. Mueller H, B. H., Bamberg E (2000). "Adsorption of Membrane-Associated Proteins to Lipid Bilayers Studied with an Atomic Force Microscope: Myelin Basic Protein and Cytochrome." J. Phys. Chem B 104: 4552-4559.

19. Richter R, B. A. (2005). "Following the Formation of Supported Lipid Bilayers on Mica: A study Combining AFM, QCM-D, and Ellipsometry." Biophysical Journal 88: 3422-3433.

20. Richter R, M. A., Brisson A (2003). "Pathways of Lipid Vesicle Deposition on Solid Surfaces: A combined QCM-D and AFM Study." Biophysical Journal 85: 3035-3047.

21. Richter R, B. R., B. A. (2006). "Formation of Solid-Supported Lipid Bilayers: An Integrated View." Langmuir 22: 3497-3505.

22. Sackmann E (1996). "Supported Membranes: Scientific and Practical Applications." Science, New Series 271: 43-48.

23. Salditt T, L. C., Spaar A, Mennicke U (2002). "X-ray reflectivity of solid-supported, multilamellar membranes." The European Physical Journal E 7: 105-116.

24. Schneider J, B. W., Lee GU (2003). "Nanometer Scale Surface Properties of Supported Lipid Bilayers Measured with Hydrophobic and Hydrophilic Atomic Force Microscope Probes." Langmuir 19: 1899-1907.

25. Schneider J, D. Y., Barger W, Lee GU (2000). "Atomic Force Microscope Image Contrast Mechanisms on Supported Lipid Bilayers." Biophysical Journal 79: 1107-1118.

26. Schonherr H, J. J., Lenz P, Frank CW, Boxer SG (2004). "Vesicle Adsorption and Lipid Bilayer Formation on Glass Studied by Atomic Force Microscopy." Langmuir 20: 11600-11606.

27. Schuy S, J. A. (2006). "Microstructuring of phospholipid bilayers on gold surfaces by micromolding in capillaries." Journal of Colloid and Interface Science 295: 93-99.

28. Seantier B, B. C., Felix O, Decher G (2004). "In Situ Investigations of the Formation of Mixed Supported Lipid Bilayers Close to the Phase Transition Temperature." Nano Letters 4: 5-10.

29. Shao Z, Y. J. (1995). "Progress in high resolution atomic force microscopy in biology." Q Rev Biophys 28: 195-251.

30. Steinem C, G. H.-J., Janshoff A (2000). "Interaction of melittin with solid supported membranes." PCCP 2: 4580-4585.

31. Tawa K, M. K. (2005). "Substrate-Supported Phospholipid Membranes Studied by Surface Plasmon Resonance and Surface Plasmon Fluorescence Spectroscopy." Biophysical Journal 89: 2750-2758.

32. Wong JY, P. C., Seitz M, Israelachvili J (1999). "Polymer-Cushioned Bilayers. II. An Investigation of Interaction Forces and Fusion Using the Surface Forces Apparatus." Biophysical Journal 77: 1458-1468.

33. Zhang L, G. S. (2005). "Slaved diffusion in phospholipid bilayers." PNAS 102: 9118-9121.